Dahl hysteresis modeling and position control of piezoelectric digital manipulator. Supplementary material

Gerardo Flores, *Member, IEEE*, and Micky Rakotondrabe, *Member, IEEE*

SIMULATION STUDY

The simulation environment is Matlab Simulink with 30 seconds of simulation time and an automatic solver with variable-step.

The system parameters used for simulation correspond to those of Table I. At the same time, the control parameters are described in Table II.

TABLE I: Set of system parameters used in the simulation. The super-index $(\cdot)^n$ means nominal value.

Parameter	Value	Parameter	Value
m_p (g)	$m_p^n = 0.1828$	c_p (N/s/m)	$c_p^n = 2.5973 \times 10^3$
d_p (N/V)	$d_p^n = 0.0468$	k_p (N/m)	$k_p^n = 2.6065 \times 10^4$
γ	$\gamma^n = 0.01$	α	$\alpha^n = 1.1773 \times 10^6$
β	$\beta^n = 121.9874$		

TABLE II: Set of control parameters used in the simulation.

Parameter	Value	Parameter	Value
l_1	2×10^3	ϵ	0.0001
l_2	1×10^6	k_1	25
l_3	3×10^5	k_2	14
l_4	0.1		

The desired trajectory is $x_1^d = 80 \sin \frac{2\pi}{10} t$ with first-time and second derivatives, $\dot{x}_1^d = x_2^d$ and $\ddot{x}_1^d = \dot{x}_2^d$, respectively. The unknown exogenous force $F(t)$ is chosen as,

$$F(t) = 50e^{-0.08(t-0.03)}\mathcal{H}(t-6) + 100 \\ 80e^{(-0.05(t-1))}\mathcal{H}(t-12) + 56e^{(-0.03(t-1.3))}\mathcal{H}(t-22), \quad (1)$$

where $\mathcal{H}(\cdot)$ is the Heaviside step function. A picture of $F(t)/m_p$ is depicted in Fig. 3.

The closed-loop system tracking error under the effect of the proposed control $u(\hat{x}_1, \hat{x}_2, \hat{\Delta})$ is depicted in Fig. 1. There are slight differences near zero in finite points due to the minor differences in the unknown signal Δ and its estimate $\hat{\Delta}$.

Besides, the observer errors (e_1, e_2) are depicted in Fig. 2. Notice how the high-gains l_1, l_2 produce a rapid convergence to zero. The unknown term $\Delta(x,t) = -\frac{\gamma}{m_p} \operatorname{sgn}(x_2)z - \frac{1}{m_p}F(t)$ and its estimate with the proposed observer is depicted in Fig. 3, where it is shown that despite the abrupt changes the convergence is achieved.

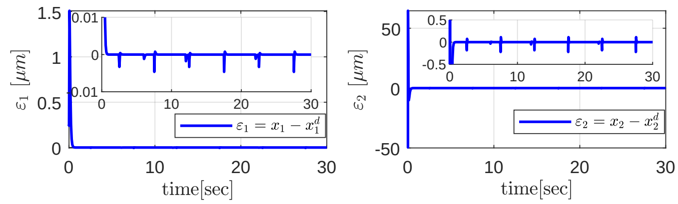

Fig. 1: The tracking errors $(\varepsilon_1, \varepsilon_2)$ under the proposed control and a zoom near zero. Recall that only $y = x_1$ is the only available output.

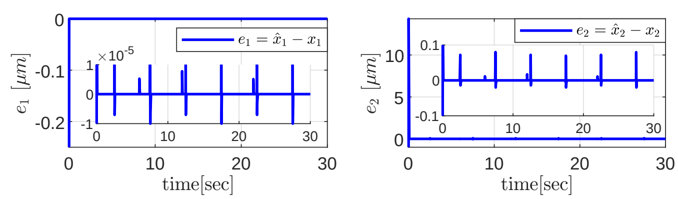

Fig. 2: The observer errors (e_1, e_2) and a zoom near zero. The error magnitude can be minimized by choosing higher gains.

Finally, the control response $u(\hat{x}_1, \hat{x}_2, \hat{\Delta})$ is depicted in Fig. 4. In the same figure, the closed-loop response map, y vs. y_d, shows a perfectly linear response, as expected.

Remark 1. *Notice that the proposed observer does not include any term that produces discontinuous solutions. Thus, the observer solution is continuously differentiable. Although it is clear that the Δ has finite discontinuous points due to the term $-\frac{\gamma}{m_p} \operatorname{sgn}(x_2)z$ in subsystem Σ_1, the observer solutions remain continuously differentiable as it can be seen in Fig. 5. Therefore, from the above discussion, it is clear that the proposed control law $u(\hat{x}_1, \hat{x}_2, \hat{\Delta})$ is also smooth. Accordingly, we include a zoom of it in Fig. 6.*

Remark 2. *External disturbance always affects the tracking error. However, such an impact can be minimized by choosing high gains in the observer, thus achieving a close estimate of Δ. We tuned the observer gains to get an estimate $\hat{\Delta}$ as close as possible to Δ, as seen in Fig. 5. Notwithstanding the above, there is always a transient response in the tracking error, as depicted in Fig. 7.*

Besides, there is always a slight difference in the tracking error, as depicted in Fig. 8. This is due to the slight error in the convergence of the estimated $\hat{\Delta}$.

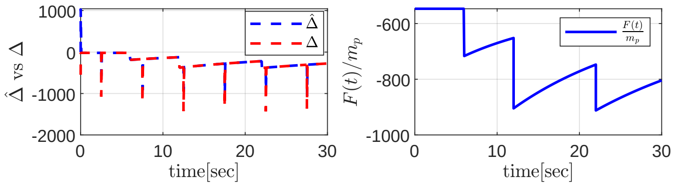

Fig. 3: On the LHS is the unknown term $\Delta(x,t)$ and its estimate $\hat{\Delta}$ obtained with the proposed observer. On the RHS is the unknown exogenous force $F(t)/m_p$ in subsystem Σ_1.

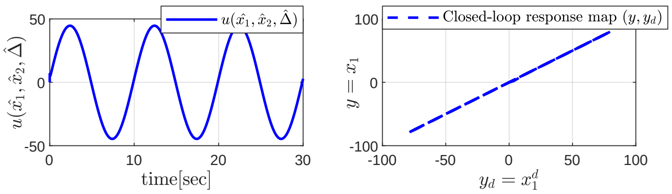

Fig. 4: The control algorithm described by $u(\hat{x}_1, \hat{x}_2, \hat{\Delta})$, and the closed-loop response map showing a clear linear behavior.

A. Comparison with state-of-the-art controllers

For a fair comparison with a PID controller, notice that we need the information of states $[x_1,\ x_2]^\intercal$ in Σ_1. However, we only have $y = x = x_1$ available for feedback. Thus, respecting the conditions of Problem 1, we only can implement a P or a PI controller. The P controller makes that the closed-loop equilibrium point $[\varepsilon_1,\ \varepsilon_2]^\intercal$ does not achieve stability due to the unknown signal Δ in Σ_1. Besides, the desired trajectory is not achieved, and the tracking error magnitude grows when the magnitude of the unknown force F in Σ_1 also grows. In our proposed controller, F, together with the hysteresis term, are in Δ. We get an estimate of it given by $\hat{\Delta}$ with the proposed observer, and then it is compensated with the output-feedback control $u(\hat{x}_1, \hat{x}_2, \hat{\Delta})$.

Notice that we could implement a mixture of our proposal, taking our observer and a PID controller using the estimated states for feedback. However, we would be using part of our result in that case, and the comparison would not be fair. Please notice that the same applies to other approaches that use the entire state for feedback, such as sliding mode control (SMC).

Notwithstanding the previous discussion, by using our proposed observer to get the estimates of $(\hat{x}_1, \hat{x}_2)$, we compared the proposed control performance with the PID and SMC. The PID is given by:

$$u_{\text{PID}} = \frac{m_p}{d_p}\left(-k_p[\hat{x}_1 - x_1^d] - k_d[\hat{x}_2 - x_2^d] - k_i\int_{t_0}^{t}[\hat{x}_1 - x_1^d]dt\right)$$

where k_p, k_d, and k_i are positive gains. While the SMC is given by,

$$\sigma = [\hat{x}_1 - x_1^d] + \alpha_1[\hat{x}_2 - x_2^d] + \alpha_2\int_{t_0}^{t}[\hat{x}_1 - x_1^d]dt,$$

$$u_{\text{SMC}} = \frac{m_p}{d_p}\left(-\beta\,\text{sgn}\,(\sigma) + \frac{k_p}{m_p}\hat{x}_1 + \frac{c_p}{m_p}\hat{x}_2 + \dot{x}_2^d\right),$$

where β, α_1, α_2 are positive gains and σ is the sliding surface. The rest of the parameters are the same system parameters defined in the paper. For the comparison, we carefully tuned

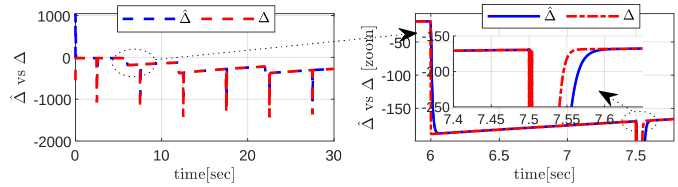

Fig. 5: On the LHS is the unknown term $\Delta(x,t)$ and its estimate $\hat{\Delta}$ obtained with the proposed observer. On the RHS is a zoom of the same signals. Notice that although Δ has some high-frequency parts, the $\hat{\Delta}$ closely smoothly approximates Δ.

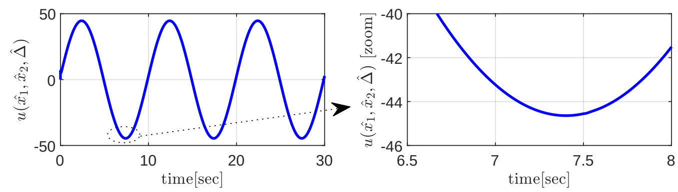

Fig. 6: The control algorithm described by $u(\hat{x}_1, \hat{x}_2, \hat{\Delta})$, and a zoom of it. From the figure, it is clear that the control law is smooth. The right-hand terms of the proposed observer and controller can corroborate this claim.

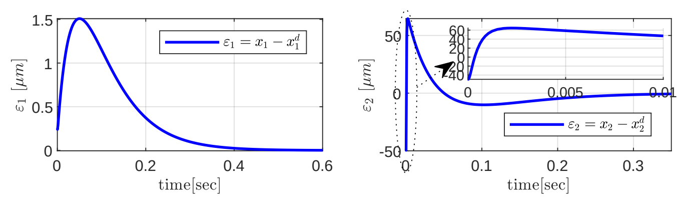

Fig. 7: The transient response of the the tracking errors $(\varepsilon_1, \varepsilon_2)$ under the proposed control.

all the above gains to find an approach to their optimal value in which the tracking error is minimized. This review depicts the adjusted control gains in Table III. The observer gains remain the same as those in the paper.

For the comparison, we used the tracking error

$$\varepsilon_1 = x_1 - x_1^d, \quad \varepsilon_2 = x_2 - x_2^d.$$

We compute its Euclidean norm together with its corresponding integral defined as,

$$\|\varepsilon\| = \sqrt{\varepsilon_1^2 + \varepsilon_2^2}, \qquad \int_{t_o}^{t}\|\varepsilon\|d\tau \tag{2}$$

respectively. The simulation results are depicted in Fig. 9. Notice that although we use part of our result (the observer), the proposed control error is minimal w.r.t. the PID and SMC. Also, we can see the chattering in Fig. 9 caused by SMC. This

TABLE III: The chosen PID and SMC parameters for comparison purposes.

PID control		SMC	
Parameter	Value	Parameter	Value
k_p	k_1k_2+1	β	5×10^3
k_d	k_1+k_2	α_1	3
k_i	$0.001k_1$	α_2	1

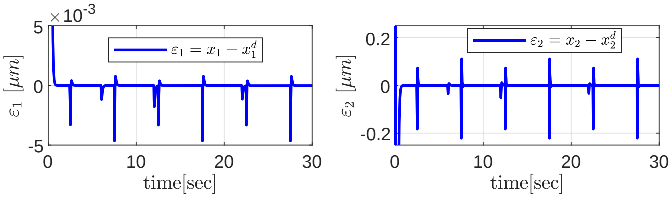

Fig. 8: This figure shows a zoom in the tracking errors $(\varepsilon_1, \varepsilon_2)$ under the proposed control. Notice that the errors do not perfectly converge to zero due to the slight error in the estimated unknown signal Δ; this can be seen in this review in Fig. 5.

is undesirable, and this kind of control is not recommended for mechanical systems like the piezoelectric digital manipulator presented in this paper. The constant oscillations in the PID, and thus its growing error integral, are due to the lack of compensation error in the unknown term; despite the integral term in the PID control.

To see the error magnitude of our proposed control, we include Fig. 10. Notice that $\|\varepsilon\|$ is practically zero almost everywhere, except in the finite number of points in which $-\frac{\gamma}{m_p}\operatorname{sgn}(x_2)z = 0$ and where the exogenous disturbance is discontinuous.

In conclusion, standard feedback controllers cannot be implemented since the only available output is $y = x_1$. To cope with that situation, we implement our proposed observer and get estimates $(\hat{x}_1, \hat{x}_2)$ used to implement the PID and SMC controls. The simulations demonstrated that our proposed controller outperforms those controllers.

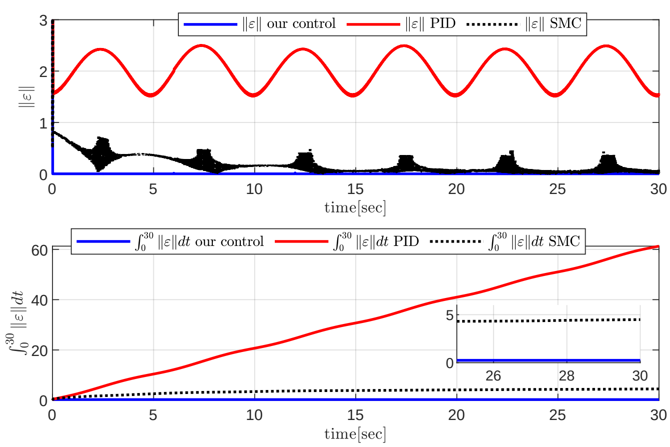

Fig. 9: Comparison with the PID and SMC. We used the norm of the vector tracking error and its corresponding integral. Notice the chattering of the SMC. The growing error integral of the PID control is mainly due to a constant oscillation in the norm of the error.

B. Control performance under system parameter variations

Notice that we have varied the values of each system parameter from -35% to $+40\%$. For that, we consider that we only know the nominal values, and thus, we used them in the control and observer. In Fig. 11 are depicted the norm of the tracking error $\|\varepsilon\|$ and the integral in which $\varepsilon = [\varepsilon_1,\ \varepsilon_2]^\intercal$. The results are satisfactory. However, we can notice a slight difference between the errors of the control with variation in the system parameters and the errors with previous knowledge in the parameters depicted in Fig. 10. Notwithstanding, the errors are even minor against the PID and SMC depicted in Fig. 9. Another difference that we can see is the ramp in the term $\int_0^{30}\|\varepsilon\|dt$. Notice that in the case of the control with perfect knowledge of the parameters, there is no ramp; please see Fig. 10. The ramp is due to a slight oscillatory error around zero in the observer, particularly in error e_2 due to parameter variations.

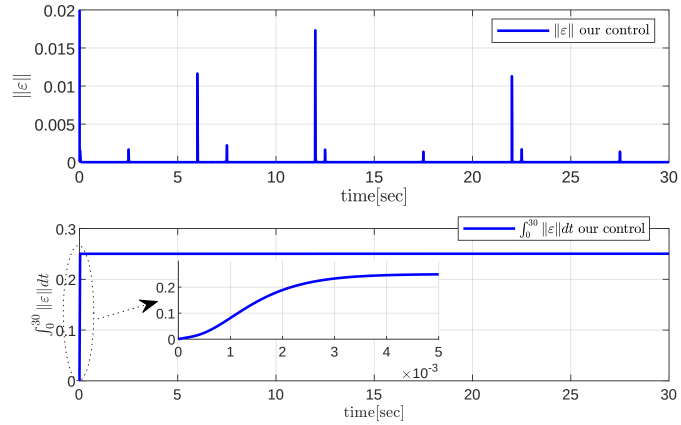

Fig. 10: This figure shows the norm of the vector tracking error and the corresponding integral of our proposed control. As discussed in response to comment R3.0, the signals are smooth, and the apparent peaks are due to the slight errors of the term $e_3 = \hat{\Delta} - \Delta$.

TABLE IV: Set of system parameters used in the simulation for the case of constant parameter variations. The nominal values denoted by $(\cdot)^n$ are those in Table I in the paper.

Parameter	Value	Parameter	Value
m_p (g)	$0.7 \times m_p^n$	c_p (N/s/m)	$0.75 \times c_p^n$
d_p (N/V)	$1.1 \times d_p^n$	k_p (N/m)	$1.1 \times k_p^n$
γ	$1.15 \times \gamma^n$	α	$0.65 \times \alpha^n$
β	$1.4 \times \beta^n$		

From the above simulations, notice that our control is robust against constant parameter variations. One of the cons, in this case, is that we should tune the control and observer parameters; however, this is normal since the parameter variation always affects the control response.

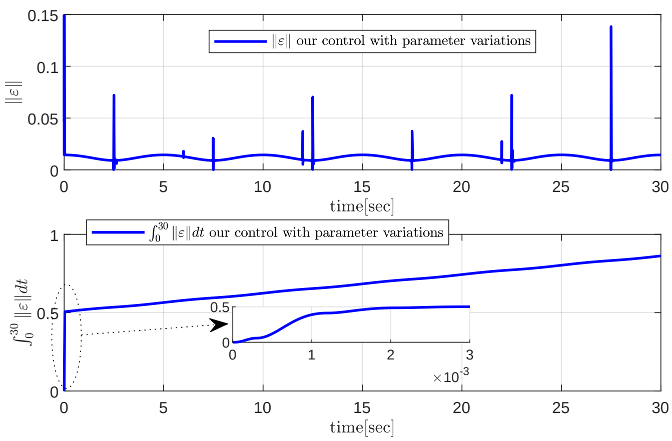

Fig. 11: Norm of the vector tracking error and the corresponding integral of our proposed control under parameter variations.